

1 **Unbiased intestinal single cell transcriptomics reveals previously uncharacterized enteric nervous  
2 system populations in larval zebrafish**

3 L.E. Kuil<sup>1,2</sup>, N. Kakialatu<sup>1</sup>, J.D. Windster<sup>1,3</sup>, E. Bindels<sup>4</sup>, J.T.M. Zink<sup>4</sup>, G. van der Zee<sup>1</sup>, R.M.W. Hofstra<sup>1</sup>, I.T. Shepherd<sup>5</sup>, V.  
4 Melotte<sup>1,6</sup> and M.M. Alves<sup>1,7</sup>

5 <sup>1</sup>Department of Clinical Genetics, Erasmus University Medical Center, Sophia Children's Hospital, Rotterdam, The  
6 Netherlands.

7 <sup>2</sup>Division of Psychosocial Research and Epidemiology, The Netherlands Cancer Institute, Amsterdam, The Netherlands.

8 <sup>3</sup>Department of Pediatric Surgery, Erasmus University Medical Center, Sophia Children's Hospital, Rotterdam, The  
9 Netherlands.

10 <sup>4</sup>Department of Hematology, Erasmus MC, Rotterdam, The Netherlands.

11 <sup>5</sup>Department of Biology, Emory University, Atlanta, Georgia, United states of America.

12 <sup>6</sup>Department of Pathology, GROW-School for Oncology and Developmental Biology, Maastricht University Medical Center,  
13 Maastricht, The Netherlands.

14 <sup>7</sup>Corresponding author: m.alves@erasmusmc.nl

15

16 **Abstract**

17 The enteric nervous system (ENS) regulates many gastrointestinal functions including  
18 peristalsis, immune regulation and uptake of nutrients. Defects in the ENS can lead to severe  
19 enteric neuropathies such as Hirschsprung disease (HSCR), which is caused by defective  
20 ENS development. Zebrafish have proven to be fruitful in the identification of novel genes  
21 involved in ENS development and HSCR pathology. However, the composition and  
22 specification of enteric neurons and glial subtypes of the larval zebrafish at a single cell level,  
23 remains mainly unexplored. Here, we performed single cell RNA sequencing of zebrafish  
24 ENS at 5 days post-fertilization. We identified both vagal neural crest progenitors and  
25 Schwann cell precursors, as well as four clusters of early differentiated neurons.  
26 Interestingly, since we took an unbiased approach where we sequenced total intestines, an  
27 *elavl3+/phox2bb-* population of neurons and the presence of *cx43+/phox2bb-* enteric glia  
28 were identified in larval zebrafish. These populations have not been described before.  
29 Pseudotime analysis supported binary neurogenic branching of ENS differentiation, which  
30 happens via a notch-responsive state. Together, our data revealed previously unrecognized  
31 ENS populations and serve as a resource to gain new insights on ENS development and  
32 specification, proving that the zebrafish is a valuable model organism in the quest towards  
33 understanding and treating congenital enteric neuropathies.

34

35 **Keywords: enteric glia; danio rerio; ENS; hirschsprung disease; HSCR**

36 **Introduction**

37 The enteric nervous system (ENS) consists of neurons and glia that are tightly  
38 interconnected together, and with cells in their microenvironment. The function of the ENS  
39 extends far beyond regulating peristalsis, as it is also involved in secretion, immune  
40 regulation and nutrient absorption, via connections with other cell types in the intestine (1). It  
41 is well known that dysregulation of ENS development leads to life-threatening congenital  
42 enteric neuropathies, of which Hirschsprung disease (HSCR) is the most common disorder,  
43 affecting approximately 1 in 5.000 live births (1, 2). ENS development occurs early during  
44 embryogenesis with vagal and sacral neural crest contributions. Recently, it has been found  
45 in mice that at postnatal stages, the ENS is supplemented by enteric neurons derived from  
46 Schwann cell precursors (SCPs) (3). This suggests that there is a dual origin of ENS cells,  
47 namely those derived from embryonic (vagal) neural crest during early gut colonization, and  
48 those derived postnatally from SCPs (3).

49 One of the vertebrate animal models that is regularly used to study ENS  
50 development, is the zebrafish (4). Zebrafish are highly suitable for genetic manipulation,  
51 develop rapidly, ex-utero and are transparent, which makes them extremely valuable for  
52 screening novel disease genes and tracing developmental processes (5, 6). However, the  
53 precise composition and specification of different neuronal and glial subtypes in the zebrafish  
54 ENS, remains unclear. This holds true particularly at larval stages, in which key processes  
55 take place to ensure proper gut colonization with enteric neurons and glia. To date, a few  
56 immunohistochemistry studies investigating enteric neuronal identities in larval zebrafish,  
57 have reported the presence of vasoactive intestinal peptide (VIP), pituitary adenylate  
58 cyclase-activating peptide (PACAP), neuronal nitric oxide synthase (nNOS), serotonin (5-  
59 hydroxytryptamine; 5HT), calretinin (CR) and calbindin (CB), from 3 days post fertilization  
60 (dpf) onwards (7, 8). Recently, it has also been described that the adult zebrafish intestine  
61 contains enteric glia, similar to that observed in mammals (9). The study showed the presence  
62 of enteric glia presenting with neurogenic properties in the adult intestine, which could be  
63 detected by the notch reporter line *her4.3:GFP* (9). However, the existence of enteric glia in  
64 larval zebrafish, is still a controversial subject. Three papers reported contradicting findings  
65 regarding expression of canonical glial genes such as *gfap*, the traditional marker for enteric  
66 glia in human and mouse. Baker *et al.* showed Gfap+ enteric glia in the outer layer of the  
67 intestine of 7 and 18 dpf fish, encapsulated by a layer of enteric neurons (10). Transmission  
68 electron microscopy showed the presence of granular vesicles and filiform processes  
69 wrapping the muscularis and caveolae, which are typical characteristic of glia (10). McCallum  
70 *et al.* also showed Gfap+ staining in the larval intestine, but suggested that the  
71 immunostaining was aspecific, since it remained in the intestine of the *ret* mutant HSCR

72 model, which lacks an ENS (9). Moreover, they showed that other typical enteric glial genes  
73 were not expressed in the zebrafish intestine, including *bfabp* (*fabp7a*), *sox10* and *s100b* (9).  
74 Such findings were supported by El-Nachef and Bronner, who reported the absence of  
75 enteric glia expressing *sox10*, *gfap*, *plp1a* and *s100b* in larval stages (11).

76 To gain new insights into the exact ENS composition of larval zebrafish, studies at the  
77 single cell transcriptome level are warranted. Previous zebrafish single cell transcriptomic  
78 studies described, did not capture enough neuronal cells for sub-analysis, or were done at  
79 very young embryonic and larval stages, showing limited neuronal specification (12-14).  
80 Here, we report single cell RNA sequencing (scRNA-seq) of 5 dpf zebrafish intestines.  
81 Importantly, we used an unbiased approach, dissecting whole intestines and sequencing all  
82 live cells without enrichment for specific ENS markers, such as *sox10* and/or *phox2bb*. Such  
83 approach allowed detection of previously unrecognized neuronal and glial populations in the  
84 larval intestine, expanding our understanding of the ENS composition and specification in  
85 larval zebrafish.

86 **Results**

87 **Vagal derived ENS cells are complemented by Schwann cell precursors (SCPs),  
88 supporting the dual origin of the ENS in zebrafish**

89 To enable capturing of the ENS from 5-day-old tg(*phox2bb*:GFP) larvae (15), 244 intestines  
90 were pooled to perform 10x scRNA-seq. Based on expression of canonical markers, as well  
91 as markers obtained in previous literature (16-18), we selected clusters that most likely  
92 contained neural crest progenitors, enteric neurons and glia (e.g. expression of *phox2bb*,  
93 *elval3/4*, *sox10*, *slc1a2b*) (n = 1369 cells; 15% of total cells) (Fig S1). Subset analysis of  
94 these cells, led to eleven distinct clusters (Fig 1A, 1B). Two of these clusters were  
95 characterized by shared expression of typical neural crest markers such as, *sox10*, *foxd3*  
96 and *phox2bb* and were therefore, classified as progenitor cells (Fig S2A). However, while  
97 one cluster selectively expressed genes typical for oligodendrocyte precursor cells (OPCs) or  
98 Schwann cell precursors (SCPs), including *clic6*, *tppp3*, and *anxa1a* (16, 19-22) (n = 50 cells;  
99 Fig 1B, S2B), the other cluster showed specific expression of more traditional (vagal) neural  
100 crest genes, such as *ret*, *hoxb5b*, and *tlx2* (23-26) (n = 181 cells; Fig 1B, S2C). *Mmp17b*,  
101 which has been described in migrating trunk neural crest and in Schwann cells upon injury,  
102 was specifically identified in the SCP cluster (Fig S2B) (20, 27, 28). We then performed  
103 single molecule fluorescent whole mount in-situ hybridization (smFISH) using a probe  
104 targeting *mmp17b*, to localize these cells in 5 dpf zebrafish and determine if they are  
105 specifically present in the gut. As expected, positive cells were present in the spinal cord and  
106 in the axonal motor neuron branches, corresponding to the known localization of SCPs (Fig

107 1C) (20, 29, 30). In the intestine, *mmp17b* signal was also observed, occasionally co-  
108 localizing with the *tg(phox2bb:GFP)* signal (Fig 1D). This signal was sparse, which is in line  
109 with our scRNA-seq data, where the majority of *mmp17b* positive cells (32 out of 52 cells)  
110 showed only 1 or 2 RNA counts/cell. Therfore, our results confirm the presence of SCPs in  
111 the zebrafish intestine, and support the rare nature of these cells at 5dpf.

112 **The zebrafish intestine contains four types of differentiated neurons at larval stage**  
113 Based on our analysis, four types of ‘differentiated neurons’ were identified. The largest  
114 cluster (n = 269 cells) consisted of inhibitory motor neurons, expressing *vip* and *nos1* (Fig  
115 1B, 2A) (31, 32). This cluster also included cells expressing *slc6a4b*, *tph1b* and *ddc*, which  
116 are genes involved in serotonin transport and production (Fig S3D-F) (33-35). Sensory  
117 intrinsic primary afferent neurons (IPANs) were identified by expression of *nmu*, *vgf*, *tac3a*  
118 and *callb2a* (n = 109 cells; Fig 1B, 2A, S3A) (32, 36). A third cluster expressing *isl2a/b*, *olig2*  
119 and *neurod1*, most likely represents motor neurons (n = 25 cells; Fig 1B, 2A, S3B) (37-39).  
120 The fourth cluster seems to contain a mix of different neuronal subtypes such as,  
121 glutamatergic, GABAergic and IPANs (n = 110 cells), based on their selective expression of  
122 *vglut2a* (*slc17a6b*), *gad1b*, *sv2a*, *neurod6*, *gad2* and *cdh8* (Fig 2A, 2B, S3C) (32, 40, 41).  
123 Interestingly, this latter cluster did not express the neural crest marker *phox2bb* (Fig 2B).

124 **Identification of a *phox2bb*- population of differentiated enteric neurons**

125 To confirm the presence of *phox2bb*- neurons in the zebrafish intestine, we first showed co-  
126 localization of the *tg(vglut2:loxP-dsRed-loxP-GFP)* and the *tg(gad1b:GFP)* reporter lines in  
127 the intestine (Fig 2C). Subsequently, we crossed the *tg(phox2bb:GFP)* reporter with the  
128 *tg(vglut2:loxP-dsRed-loxP-GFP)* reporter and found no co-localization between *phox2bb* and  
129 *vglut2* *in vivo*, confirming the presence of *phox2bb*-/*vglut2a* cells in the zebrafish intestine  
130 (Fig 2D). Our transcriptomic data also showed that these cells express *elavl3* (encoding  
131 HuC; Fig 2B), which led us to perform a HuC/D staining on 5 dpf *tg(phox2bb:GFP)* fish. We  
132 observed that a limited number (between 0 to 25) of HuC/D+;*phox2bb*- cells were present in  
133 the zebrafish intestine, comprising on average 2.5% of the total ENS (Fig 3A). This number,  
134 roughly corresponds to our scRNA-seq data (8% of total ENS cells). Distribution of  
135 HuC/D+;*phox2bb*- cells seems equal along the anterior to posterior axis, indicating that these  
136 cells are evenly distributed along the total length of the intestine and therefore, do not seem  
137 to be region specific (Fig 3A).

138

139 **Larval zebrafish intestine contains enteric glia**

140 Although recent compelling evidence suggest the presence of enteric glia in the adult  
141 zebrafish intestine (9), previous studies are unambiguous about the existence of these cells  
142 in larval zebrafish. This is mainly due to the absence of expression markers typical for this

143 cell type in mice and humans. In line with previous reports, our data confirmed the absence  
144 of *gfap*+ cells in the larval intestine of the tg(*gfap*:GFP) reporter line (Fig S4C). However, due  
145 to our unbiased approach of sequencing total intestines, we were able to observe a cluster of  
146 cells lacking expression of *phox2bb* and *sox10*, but expressing Hairy/E(spl)-related 4 (*her4*)  
147 genes (n = 30 cells; Fig S4A). Interestingly, this cluster showed highly specific expression of  
148 genes typically found in radial glia in the zebrafish brain, such as *glula*, *slc1a2b* and *ptn* (16),  
149 and of genes expressed in mammalian enteric glia, such as *cx43*, *s100b*, *sox2*, *ptprz1b*, and  
150 *fabp7a* (Fig 3B, S4B) (42-46). Analysis of tg(*her4*:GFP);tg(*phox2bb*:kaede) larvae showed  
151 that *her4*+/*phox2bb*- cells are indeed present in the intestine and are located in close  
152 proximity to, or in some cases in direct contact to, *phox2bb*+ cells (Fig 3C). To validate the  
153 enteric glial identity of these cells, we performed immunohistochemistry on tg(*phox2bb*:GFP)  
154 larvae at 3, 4, 6 and 10 dpf using an antibody against connexin 43 (Cx43), a known enteric  
155 glia marker in mice that we found expressed in the Cx43+/*phox2bb*- cluster. Based on our  
156 results, Cx43+ cells were detected from 4 dpf onwards, suggesting that enteric glia arise  
157 between 3 and 4 dpf in zebrafish (Fig 4A). At 4 dpf, Cx43+ cells were most often observed in  
158 the middle intestinal segment, with an average of 12 cells per fish (Fig 4B). Although the  
159 location of Cx43+ cells is similar to *phox2bb*+ cells, as they were often observed in the same  
160 focal plane in close proximity to each other, these cells were always negative for the  
161 *phox2bb* reporter.

162

### 163 **Progenitor cells become notch-responsive before differentiation towards neuronal and 164 glial fate**

165 RNA expression of a marker for differentiated neurons, *elavl3*, and a gene specific for early  
166 neural crest/progenitor cells, *sox10*, showed that these genes are expressed exclusively on  
167 the left and right side of the UMAP, respectively. Analysis of key cell fate mediators for pan-  
168 neurogenic fate (e.g. *elavl4* and *insm1b*) or genes expressed in newborn neurons in the  
169 zebrafish brain (e.g. *tubb5* and *tmsb*), showed a similar pattern of expression on the left side  
170 of the UMAP (Fig S5A) (16). This suggests a trajectory of progenitors' differentiation towards  
171 neurons, from right to left in the UMAP. Pseudotime analysis by monocle3 (47) confirmed  
172 this differentiation trajectory and additionally showed that during differentiation, a bifurcation  
173 into two types of early differentiated neurons occurs, branch 1: sensory IPANs versus branch  
174 2: inhibitory motor neurons (Fig 4C). This latter branch also contains a secondary branch  
175 towards serotonergic neurons (see asterix in Fig. 4C). In line with this finding, Morarach et al.  
176 reported a similar bifurcation in the murine ENS differentiation trajectory, with branch A,  
177 forming Vip/Nos positive neurons (32). Expression of "branch A marker genes" *etv1* and  
178 *ebf1a*, was also found in our dataset, in the *vip*+/*nos1*+ inhibitor motor neuron branch (Fig  
179 4C, S5C). Conservation in expression of various genes at specific differentiation states is

180 depicted in figure 4 panel C (32). Comparing our data to the dataset from Howard *et al.*  
181 showed that the early differentiation observed in zebrafish from 68-70 hours post fertilization  
182 (hpf), is prominently seen in our dataset (14). For example, co-expression of *slc18a2* and  
183 *pbx3b* was observed in differentiated neurons including IPANs (Fig 4C).

184 Our data also showed that neuronal differentiation seems to start in notch-responsive  
185 cells, specifically expressing *notch1a*, *notch3* and notch-responsive *her4* genes (Fig S5B)  
186 (9). In line, our UMAP showed co-expression of the known cell fate mediator gene *sox11a*,  
187 and notch (responsive) genes (Fig S5B) (16). Live-imaging of 5 dpf  
188 *tg(her4:GFP)/tg(8.3phox2bb:keade)* fish showed that a subset of *phox2bb*+ cells is indeed  
189 *her4*+ (15% of cells in the posterior intestine), confirming the presence of *phox2bb*/*her4*+  
190 notch responsive cells *in vivo* (Fig 4D). Thus, progenitor cells seem to become notch  
191 responsive upon initiation of differentiation towards neurons (branch 1 and 2). In addition,  
192 there is a third trajectory emanating progenitors towards clusters containing proliferative  
193 cells, motor neurons and enteric glia, suggesting a separate differentiation route towards a  
194 cycling/enteric glial fate (Fig 4C).

195

## 196 **Discussion**

197 Here, we present for the first time a single cell atlas of the ENS of 5 dpf zebrafish. Our results  
198 show the presence of two clusters of progenitor cells, traditional vagal neural crest cells and  
199 Schwann cell precursors (SCPs), confirming a dual origin of the zebrafish ENS. Based on  
200 our dataset, we were able to identify *mmp17b* as a specific marker for SCPs, and were able  
201 to confirm the presence of these cells in the gut, as well as their rare nature *in vivo*. Our data,  
202 also showed the presence of four clusters of enteric neurons and a cluster of enteric glia, at  
203 this developmental stage. Inhibitory motor neurons were confirmed to be major contributors  
204 of the zebrafish ENS (7, 8), but we were also able to identify other differentiated neuronal  
205 subtypes. We can clearly see that early enteric neuronal differentiation occurs as an initial  
206 bifurcation towards two major branches. Differentiation of sensory IPANs seem to develop  
207 via branch 1, whereas *vip*+/*nos1*+ inhibitory motor neurons specify via branch 2. The latter,  
208 seems to contain a secondary branch towards serotonergic enteric neurons. Therefore,  
209 differentiation of enteric inhibitory motor neurons as well as serotonergic neurons, seems to  
210 be conserved between at least, mice and zebrafish (32). Interestingly, due to our unbiased  
211 sequencing approach in which the whole intestine was analysed, we were able to identify  
212 one cluster of *elavl3*+/*phox2bb*- differentiated neurons, expressing genes specific for  
213 glutamatergic neurons, GABAergic neurons, and others involved in serotonergic signaling.  
214 Based on our live imaging data, *elavl3*+/*phox2bb*- neurons are located in close proximity or  
215 sometimes even directly adjoined, to *phox2bb*+ enteric neurons. To our knowledge, such

216 population has never been defined before, as all enteric neurons were assumed to express  
217 *phox2bb*. Future lineage tracing experiments should be performed to confirm the neural  
218 crest-origin of these cells, as well as scRNA-seq experiments at older ages, to provide  
219 insights into which neuronal sub-types these *phox2bb*- cells contribute.

220 Finally, our dataset showed the presence of a cluster of enteric glial cells. In line with  
221 previous studies, we found that the relative contribution of enteric glial to the ENS seems to  
222 be less abundant in zebrafish, compared to that in human and mice. We now show that  
223 enteric glia can be detected already at zebrafish larval stages. We also confirmed that  
224 canonical enteric glial genes such as, *sox10*, and *plp1a* are not expressed in the putative  
225 enteric glial cluster. However, we did detect RNA expression of *s100b* and *fabp7a*, which is  
226 in contrast to previous studies (9, 11). In addition, we showed that canonical glia in larval  
227 zebrafish express *cx43*, *notch3* and *her* genes, but lack *phox2bb* expression. The *her4*-  
228 reporter line previously described, has specifically characterized enteric glia in the adult  
229 zebrafish intestine (9). However, here we show that only the *phox2bb*-/*her4*+ cells, but not  
230 the *phox2bb*+/*her4*+ cells, express enteric glial markers at larval stages. Interestingly, *her4*  
231 expression was not only limited to enteric glia, but was also consistently found in *phox2bb*+

232 'intermediate cells' undergoing differentiation. A previous study had already shown that  
233 enteric neural crest cells start to express *her4* after migration, and lose its expression upon  
234 differentiation (9). Here, we extended their findings by showing differentiation at a single cell  
235 transcriptional level, from progenitors via a notch responsive state, towards early  
236 specification of enteric neuronal fate. Together, this suggests that Notch signaling plays a  
237 central role in the transition from progenitor to neuronal state or glial differentiation. In line  
238 with this, disruption of Notch signaling in mice (*Pofut1* knockout), was shown to result in the  
239 absence of an ENS, confirming that this signaling pathway is crucial to maintain the neural  
240 crest progenitor pool (48). The Notch pathway has also been recognized in the maintenance  
241 of neuronal stem cells in the brain, but signaling dynamics in neuronal differentiation have yet  
242 to be elucidated (Reviewed by (49)).

243 Taken together, our results show that the zebrafish ENS has a dual origin of  
244 precursor cells, that follow specification upon notch activation towards either a neuronal fate,  
245 or via a cycling state towards an enteric glial fate. It also shows that using an unbiased  
246 approach in which cells are not selected for a specific reporter construct, can be instrumental  
247 to find new cell clusters. In summary, our data adds to the understanding of healthy ENS  
248 development and offers an essential framework for intra-study, cross-species, and disease  
249 state comparisons.

250 **Acknowledgements**

251 We want to thank Remco Hoogenboezem for mapping the scRNA-seq data, Emma de Pater  
252 for useful discussions, and the optical imaging center (OIC) of the Erasmus University  
253 Medical Center for assistance with confocal microscopy.

254 **Funding**

255 This work was funded by the friends of Sophia foundation (SSWO WAR-63).

256

257 **Figure legends**

258 **Figure 1. Single cell transcriptomics of 5 dpf zebrafish ENS**

259 A) UMAP of 1369 ENS cells, containing eleven different clusters. B) Dot plot showing  
260 expression of genes highly differentially expressed between clusters. C) smFISH of 5 dpf  
261 *tg(phox2bb:GFP)* larvae stained for *mmp17b* (magenta). Scale bar represents 50  $\mu$ m. D)  
262 Zoom images of smFISH of 5 dpf *tg(phox2bb:GFP)* larvae showing co-localization of  
263 *mmp17b* (magenta) and *phox2bb* (green) in the intestine, outlined with dotted lines. Arrows  
264 highlight cells of interest showing colocalization. Scale bar represents 10  $\mu$ m.

265

266 **Figure 2. Cluster of *elavl3+;phox2bb-* enteric neurons present with excitatory and  
267 inhibitory gene expression**

268 A) Featureplots of genes defining four clusters of differentiated neurons. B) Featureplots  
269 highlighting the presence of a cluster of cells expressing *elavl3*, *slc17a6b* and *gad1b*, but  
270 lacking expression of *phox2bb* (*phox2bb-* differentiated neurons, depicted by the circle). C)  
271 Live imaging of 7 dpf *tg(gad1b:GFP);tg(vglut2a-dsRed)* larval intestine shows overlap  
272 between the two reporters (arrows) with one *gad1b+* cell that is *vlgut2-* (arrowhead). Scale  
273 bar represents 40  $\mu$ m. D) Live imaging of 7 dpf *tg(phox2bb:GFP);tg(vglut2a-dsRed)* larval  
274 intestine shows no overlap between the two reporters. Scale bar represents 10  $\mu$ m.

275

276 **Figure 3. One small cluster expresses genes typical for enteric glia in mammals**

277 A) *HuC/D* antibody staining shows that most *HuC/D+* cells in the intestine express *phox2bb*,  
278 but also show *phox2bb+/HuC/D-* cells (progenitors) depicted by arrowheads and *phox2bb-*  
279 ;*HuC/D+* cells (differentiated neurons) depicted by arrows. Scale bar represents 40  $\mu$ m.  
280 Quantification of the relative amount of double and single positive cells are presented in pie  
281 charts (n=9). B) Featureplots showing selective expression of *cx43*, *glula*, *slc1a2b* and *s100b*  
282 in one specific cluster of enteric glia depicted by the circle. C) Live-imaging of 5 dpf  
283 *tg(8.3phox2bb:kaede);tg(her4:GFP)* intestines shows *phox2bb-;her4+* cell depicted by the

284 arrowheads that are in close proximity to, or seem to interact with *phox2bb*+ neurons. Scale  
285 bar represents 20  $\mu$ m.

286

287 **Figure 4. Pseudotime analysis shows differentiation trajectories from right to left of**  
288 **the UMAP**

289 A) Immunohistochemistry staining of Cx43 in the *tg(phox2bb:GFP)* reporter line shows non  
290 overlapping expression in the intestine. Representative images from 4 dpf larvae. Scale bar  
291 represents 40  $\mu$ m. B) Upper graph showing the percentage of larvae that contained Cx43  
292 cells in their proximal, middle and distal intestine. The lower graph shows the number of  
293 Cx43 cells per larvae in the proximal, middle and distal intestine (n=19). C) Pseudotime  
294 color-coded featureplot showing a bifurcation towards neuronal differentiation (sensory IPAN:  
295 branch1 and inhibitory motor neurons: branch2 containing a secondary branch towards  
296 serotonergic neurons marked with the asterix). D) Live-imaging of 5 dpf  
297 *tg(8.3phox2bb:kaede);tg(her4:GFP)* intestines shows *phox2bb*+/*her4*+ cells, representing  
298 cells undergoing differentiation from progenitor state towards neuronal or glial fate. Scale bar  
299 represents 20  $\mu$ m.

300

301 **Supplementary figures**

302 **Supplementary figure 1. Featureplots showing the clusters selected for subset**  
303 **analysis of the ENS**

304 A) UMAP featureplots showing the cells that are selected for subset analysis of the ENS in  
305 purple and other non-ENS cells in grey. B) Featureplots showing expression of *phox2bb*,  
306 *GFP*, *her4.1* and *elavl3* in the ENS subset.

307

308 **Supplementary figure 2. Featureplots showing specific gene expression in various**  
309 **clusters**

310 A) UMAP featureplots showing expression of genes in the clusters containing A) precursors;  
311 B) SCPs, as well as C) vagal neural crest cells and their derivatives.

312

313 **Supplementary figure 3. Featureplots showing specific expression in differentiated**  
314 **neuronal clusters**

315 UMAP featureplots showing expression of genes in the clusters containing A) sensory  
316 IPANs; B) motor neurons; C) *phox2bb*- neurons (*sv2a*+), and D) serotonergic neurons (in the  
317 inhibitory motor neurons cluster).

318

319 **Supplementary figure 4. Featureplots showing specific expression in enteric neurons**

320 A) UMAP featureplots showing the absence of expression of *phox2bb* and *sox10*, but  
321 presence of *her4* expression in the enteric glial cluster depicted by the circle. B) UMAP  
322 featureplots showing expression of genes in the enteric glial cluster, depicted by the circle.  
323 C) Live-imaging capture of the *tg(gfap:GFP)* reporter line showing the absence of GFP+ cells  
324 in the intestine, which is outlined by dotted lines. Abbreviation: AF = autofluorescence.

325

326 **Supplementary figure 5. Featureplots showing expression of genes at specific**  
327 **differentiation states**

328 A) UMAP featureplots showing expression of genes typical for cells committed to neuronal  
329 differentiation. B) UMAP featureplots showing expression of notch genes, notch responsive  
330 *her4.2.1.* and the cell fate mediator gene *sox11a*. C) UMAP featureplots showing expression  
331 of genes that define differentiation branches previously described (32).

332

333

334

335 **Material and methods**

336 **Animal husbandry**

337 The following zebrafish lines were used: transgenic tg(*phox2bb*:GFP)(15),  
338 tg(8.3*phox2bb*:keade)(50), tg(*her4*:GFP)(51), tg(*gfap*:GFP)(52), tg(*vglut2*:loxP-dsRed-loxP-  
339 GFP)(53), and tg(*gad1b*:GFP) (54). Zebrafish were kept on a 14/10h light/dark cycle.  
340 Embryos and larvae were kept in an incubator at 28.5°C in HEPES-buffered E3 medium. For  
341 imaging experiments, fish were treated from 24 hpf onwards, with 0.2 mM 1-phenyl 2-  
342 thiourea (PTU), to inhibit pigmentation. Animal experiments were approved by the Animal  
343 Experimentation Committee of the Erasmus MC, Rotterdam.

344

345 **Isolation of zebrafish intestines**

346 Intestines of 5 days post-fertilization (dpf) larvae were isolated as followed: a row of 6-10  
347 larvae anesthetized with 0,0016% Tricaine, were placed on an 1.8% agarose plate.  
348 Intestines were isolated using insect pins under a dissection microscope (Olympus SZX16),  
349 collected with a tweezer and placed in an Eppendorf tube containing phosphate buffered  
350 saline (PBS) with 10% fetal calf serum (FCS), on ice. In total 244 intestines were isolated  
351 and pooled together.

352

353 **Pre-processing of zebrafish cell suspension for scRNA sequencing**

354 Cells were dissociated using 2.17mg/mL papain dissolved in HBSS, with CaCl<sub>2</sub> and MgCl<sub>2</sub>.  
355 Papain was activated using 2.5µl cysteine (1M) and dissociation was performed in a water  
356 bath at 37°C, for 10 minutes. Cells were then transferred into a FACS tube using a 35 µm  
357 cell strainer. Cells were centrifuged at 700g for 5 minutes at 4°C, the supernatant was  
358 removed and pellets were resuspended in PBS containing 10% FCS. DAPI was added to  
359 mark dead cells (1:1000). All sorts were performed using the FACSaria III sorter, into  
360 eppendorfs containing PBS with 5% FCS.

361

362 **Single cell RNA sequencing (scRNA-seq)**

363 Single cells were barcoded using a 10x genomics Chromium Controller, and sequenced  
364 using a Novaseq 6000 instrument (Illumina). In total, 9.858 cells were sequenced with mean  
365 reads per cell of 21.106. For scRNA-seq analysis we used Seurat V3 (55). The Seurat  
366 pipeline was used for filtering (nFeature\_RNA > 100 & nFeature\_RNA <4200 & percent.mito  
367 < 0.05), normalization and downstream analysis for clustering, where we used 50  
368 dimensions with a resolution of 0.8 for the UMAP processing. This led to 49 clusters, which  
369 we annotated based on differential gene expression. Seven clusters expressing neuronal  
370 and/or enteric progenitor markers were identified (cluster 6, 10, 13, 19, 21, 23, 34)(Fig. S1).

371 These seven clusters were selected for a subset analysis, using 30 dimensions with a  
372 resolution of 0.7 for the clustering and UMAP, resulting in 14 clusters. One cluster was  
373 excluded as it contained leukocytes (*lcp1+*, *phox2bb-*, *elavl3-*, *sox10-*; cluster 12) and  
374 proliferating cells negative for *phox2bb* and *elavl3* were manually excluded. The final set was  
375 analyzed using six dimensions and a resolution of 0.4. This analysis provided us with eleven  
376 clusters, which were annotated based on the differential gene expression and literature  
377 search. If required, a more thorough analysis of the total set of differentially expressed genes  
378 per cluster, or differentially expressed genes between specific subclusters, was performed.  
379 For pseudotime analysis, monocle3 was used (47).

380

### 381 **Fluorescent imaging**

382 Imaging was performed as previously described (56). For the keade photoconversion  
383 experiments, all *phox2bb+* cells in the total intestines were photoconverted using the 405  
384 nanometer (nm) laser, as described earlier (11). After photoconversion, the green and red  
385 channels were recorded, using a sequential scan with the 488nm and 561nm lasers to  
386 confirm full photoconversion.

387

### 388 **Immunohistochemistry**

389 Whole mount immunohistochemistry using mouse anti-HuC/D (1:100, molecular probes A-  
390 21271) was performed, as previously described (57). Antibody staining using rabbit anti-  
391 Cx43 (1:200, Cell Signaling Technologies 83649) was performed as published before (58).  
392 To increase signal to noise ratio we made use of monovalent AffiniPure Fab Fragments (111-  
393 167-003 Jackson; Cy<sup>TM</sup>3 AffiniPure Fab Fragment Goat Anti-Rabbit IgG).

### 394 **Single-molecule whole-mount fluorescent *in situ* hybridization**

395 Zebrafish were fixed in 4% paraformaldehyde in PBS, overnight. They were then dehydrated  
396 through a series of 25/50/75/100% MeOH in PBST for 5 minutes each, and stored for a  
397 minimum of 1 hour at -20 °C. Next, samples were rehydrated through a series of 75/50/25/0%  
398 MeOH in PBST for 5 minutes each, and incubated in prot K for 15 minutes at 20 °C. They  
399 were rinsed twice with PBST for 5 minutes and re-fixed in 4% PFA in PBS, for 20 minutes at  
400 room temperature. Susequently, samples were rinsed again 5x5 minutes in PBST. After  
401 manual pre-treatment for permeabilization, we continued with the RNAscope Multiplex  
402 Fluorescence Reagent Kit v2 Assay (Advanced Cell Diagnostics, Bio-Techne), according to  
403 the manufacturers' instructions. A custom made probe for *dr-mmp17b* C1 (NPR-0035110)  
404 was used (Advanced Cell Diagnostics, Bio-Techne). Opal 570 dye (Akoya Biosciences) was  
405 used for channel development.

406

407

408 **References**

- 409 1. Niesler B, Kuerten S, Demir IE, Schafer KH. Disorders of the enteric nervous system - a holistic  
410 view. *Nat Rev Gastroenterol Hepatol.* 2021;18(6):393-410.
- 411 2. Duess JW, Hofmann AD, Puri P. Prevalence of Hirschsprung's disease in premature infants: a  
412 systematic review. *Pediatr Surg Int.* 2014;30(8):791-5.
- 413 3. Uesaka T, Nagashimada M, Enomoto H. Neuronal Differentiation in Schwann Cell Lineage  
414 Underlies Postnatal Neurogenesis in the Enteric Nervous System. *J Neurosci.* 2015;35(27):9879-88.
- 415 4. Kuil LE, Chauhan RK, Cheng WW, Hofstra RMW, Alves MM. Zebrafish: A Model Organism for  
416 Studying Enteric Nervous System Development and Disease. *Frontiers in Cell and Developmental  
417 Biology.* 2021;8(1874).
- 418 5. Kuil L, MacKenzie KC, Tang C, Windster J, Linh Le T, Karim A, et al. Size matters: large copy  
419 number losses reveal novel Hirschsprung disease genes. *medRxiv.* 2020:2020.11.02.20221481.
- 420 6. Davidson AE, Straquadiine NR, Cook SA, Liu CG, Ganz J. A rapid F0 CRISPR screen in zebrafish  
421 to identify regulators of neuronal development in the enteric nervous system. *bioRxiv.*  
422 2021:2021.07.17.452230.
- 423 7. Uyttebroek L, Shepherd IT, Harrisson F, Hubens G, Blust R, Timmermans J-P, et al.  
424 Neurochemical coding of enteric neurons in adult and embryonic zebrafish (*Danio rerio*). *Journal of  
425 Comparative Neurology.* 2010;518(21):4419-38.
- 426 8. Olsson C, Holmberg A, Holmgren S. Development of enteric and vagal innervation of the  
427 zebrafish (*Danio rerio*) gut. *The Journal of comparative neurology.* 2008;508(5):756-70.
- 428 9. McCallum S, Obata Y, Fourli E, Boeing S, Peddie CJ, Xu Q, et al. Enteric glia as a source of  
429 neural progenitors in adult zebrafish. *Elife.* 2020;9.
- 430 10. Baker PA, Meyer MD, Tsang A, Uribe RA. Immunohistochemical and ultrastructural analysis of  
431 the maturing larval zebrafish enteric nervous system reveals the formation of a neuropil pattern. *Sci  
432 Rep.* 2019;9(1):6941.
- 433 11. El-Nachef WN, Bronner ME. De novo enteric neurogenesis in post-embryonic zebrafish from  
434 Schwann cell precursors rather than resident cell types. *Development.* 2020;147(13).
- 435 12. Hayot G, Massonot M, Keime C, Faure E, Golzio C. *CHD8*-associated  
436 gastrointestinal complaints are caused by impaired vagal neural crest development and homeostatic  
437 imbalance. *bioRxiv.* 2021:2021.10.06.463249.
- 438 13. Willms RJ, Jones LO, Hocking JC, Foley E. A cell atlas of microbe-responsive processes in the  
439 zebrafish intestine. *Cell Rep.* 2022;38(5):110311.
- 440 14. Howard AGt, Baker PA, Ibarra-Garcia-Padilla R, Moore JA, Rivas LJ, Tallman JJ, et al. An atlas  
441 of neural crest lineages along the posterior developing zebrafish at single-cell resolution. *Elife.*  
442 2021;10.
- 443 15. Nechiporuk A, Linbo T, Poss KD, Raible DW. Specification of epibranchial placodes in  
444 zebrafish. *Development.* 2007;134(3):611-23.
- 445 16. Lange C, Rost F, Machate A, Reinhardt S, Lesche M, Weber A, et al. Single cell sequencing of  
446 radial glia progeny reveals the diversity of newborn neurons in the adult zebrafish brain.  
447 *Development.* 2020;147(1).
- 448 17. Roy-Carson S, Natukunda K, Chou HC, Pal N, Farris C, Schneider SQ, et al. Defining the  
449 transcriptomic landscape of the developing enteric nervous system and its cellular environment.  
450 *BMC Genomics.* 2017;18(1):290.
- 451 18. Elworthy S, Pinto JP, Pettifer A, Cancela ML, Kelsh RN. Phox2b function in the enteric nervous  
452 system is conserved in zebrafish and is sox10-dependent. *Mech Dev.* 2005;122(5):659-69.
- 453 19. Xia W, Zhu J, Wang X, Tang Y, Zhou P, Hou M, et al. ANXA1 directs Schwann cells proliferation  
454 and migration to accelerate nerve regeneration through the FPR2/AMPK pathway. *FASEB J.*  
455 2020;34(10):13993-4005.

456 20. Leigh NR, Schupp MO, Li K, Padmanabhan V, Gastonguay A, Wang L, et al. Mmp17b is  
457 essential for proper neural crest cell migration in vivo. *PLoS One*. 2013;8(10):e76484.

458 21. Siems SB, Jahn O, Eichel MA, Kannaiyan N, Wu LMN, Sherman DL, et al. Proteome profile of  
459 peripheral myelin in healthy mice and in a neuropathy model. *Elife*. 2020;9.

460 22. Pooyan P, Karamzadeh R, Mirzaei M, Meyfour A, Amirkhan A, Wu Y, et al. The Dynamic  
461 Proteome of Oligodendrocyte Lineage Differentiation Features Planar Cell Polarity and  
462 Macroautophagy Pathways. *Gigascience*. 2020;9(11).

463 23. Lui VC, Cheng WW, Leon TY, Lau DK, Garcia-Barcelo MM, Miao XP, et al. Perturbation of  
464 hoxb5 signaling in vagal neural crests down-regulates ret leading to intestinal hypoganglionosis in  
465 mice. *Gastroenterology*. 2008;134(4):1104-15.

466 24. Howard AGAt, Nguyen AC, Tworig J, Ravisankar P, Singleton EW, Li C, et al. Elevated Hoxb5b  
467 Expands Vagal Neural Crest Pool and Blocks Enteric Neuronal Development in Zebrafish. *Front Cell*  
468 *Dev Biol*. 2021;9:803370.

469 25. Borghini S, Bachetti T, Fava M, Di Duca M, Cargnini F, Fornasari D, et al. The TLX2 homeobox  
470 gene is a transcriptional target of PHOX2B in neural-crest-derived cells. *Biochem J*. 2006;395(2):355-  
471 61.

472 26. Borghini S, Di Duca M, Santamaria G, Vargiuoli M, Bachetti T, Cargnini F, et al. Transcriptional  
473 regulation of TLX2 and impaired intestinal innervation: possible role of the PHOX2A and PHOX2B  
474 genes. *Eur J Hum Genet*. 2007;15(8):848-55.

475 27. Prendergast A, Linbo TH, Swarts T, Ungos JM, McGraw HF, Krispin S, et al. The  
476 metalloproteinase inhibitor Reck is essential for zebrafish DRG development. *Development*.  
477 2012;139(6):1141-52.

478 28. Arthur-Farraj P, Coleman MP. Lessons from Injury: How Nerve Injury Studies Reveal Basic  
479 Biological Mechanisms and Therapeutic Opportunities for Peripheral Nerve Diseases.  
480 *Neurotherapeutics*. 2021;18(4):2200-21.

481 29. Rosenberg A, Isaacman-Beck J, Franzini-Armstrong C, Granato M. Schwann Cells and Deleted  
482 in Colorectal Carcinoma Direct Regenerating Motor Axons Towards Their Original Path. *The Journal*  
483 of neuroscience : the official journal of the Society for Neuroscience. 2014;34:14668-81.

484 30. Perlin JR, Lush ME, Stephens WZ, Piotrowski T, Talbot WS. Neuronal Neuregulin 1 type III  
485 directs Schwann cell migration. *Development*. 2011;138(21):4639-48.

486 31. Keef KD, Shuttleworth CW, Xue C, Bayguinov O, Publicover NG, Sanders KM. Relationship  
487 between nitric oxide and vasoactive intestinal polypeptide in enteric inhibitory neurotransmission.  
488 *Neuropharmacology*. 1994;33(11):1303-14.

489 32. Morarach K, Mikhailova A, Knoflach V, Memic F, Kumar R, Li W, et al. Diversification of  
490 molecularly defined myenteric neuron classes revealed by single-cell RNA sequencing. *Nat Neurosci*.  
491 2021;24(1):34-46.

492 33. Del Colle A, Israelyan N, Gross Margolis K. Novel aspects of enteric serotonergic signaling in  
493 health and brain-gut disease. *Am J Physiol Gastrointest Liver Physiol*. 2020;318(1):G130-G43.

494 34. Shih DF, Hsiao CD, Min MY, Lai WS, Yang CW, Lee WT, et al. Aromatic L-amino acid  
495 decarboxylase (AADC) is crucial for brain development and motor functions. *PLoS One*.  
496 2013;8(8):e71741.

497 35. Ren J, Isakova A, Friedmann D, Zeng J, Grutzner SM, Pun A, et al. Single-cell transcriptomes  
498 and whole-brain projections of serotonin neurons in the mouse dorsal and median raphe nuclei.  
499 *Elife*. 2019;8.

500 36. Delvalle NM, Dharshika C, Morales-Soto W, Fried DE, Gaudette L, Gulbransen BD.  
501 Communication Between Enteric Neurons, Glia, and Nociceptors Underlies the Effects of Tachykinins  
502 on Neuroinflammation. *Cell Mol Gastroenterol Hepatol*. 2018;6(3):321-44.

503 37. Catala M, Kubis N. Gross anatomy and development of the peripheral nervous system. *Handb*  
504 *Clin Neurol*. 2013;115:29-41.

505 38. Hutchinson SA, Eisen JS. Islet1 and Islet2 have equivalent abilities to promote motoneuron  
506 formation and to specify motoneuron subtype identity. *Development*. 2006;133(11):2137-47.

507 39. Memic F, Knoflach V, Sadler R, Tegerstedt G, Sundstrom E, Guillemot F, et al. *Ascl1 Is*  
508 *Required for the Development of Specific Neuronal Subtypes in the Enteric Nervous System.* *J*  
509 *Neurosci.* 2016;36(15):4339-50.

510 40. Tong Q, Ma J, Kirchgessner AL. *Vesicular glutamate transporter 2 in the brain-gut axis.*  
511 *Neuroreport.* 2001;12(18):3929-34.

512 41. Wright CM, Garifallou JP, Schneider S, Menth HL, Kothakappa DR, Maguire BA, et al. *Dlx1/2*  
513 *mice have abnormal enteric nervous system function.* *JCI Insight.* 2020;5(4).

514 42. Grubisic V, McClain JL, Fried DE, Grants I, Rajasekhar P, Csizmadia E, et al. *Enteric Glia*  
515 *Modulate Macrophage Phenotype and Visceral Sensitivity following Inflammation.* *Cell Rep.*  
516 2020;32(10):108100.

517 43. McClain J, Grubisic V, Fried D, Gomez-Suarez RA, Leinninger GM, Sevigny J, et al. *Ca<sup>2+</sup>*  
518 *responses in enteric glia are mediated by connexin-43 hemichannels and modulate colonic transit in*  
519 *mice.* *Gastroenterology.* 2014;146(2):497-507 e1.

520 44. Rao M, Gershon MD. *The bowel and beyond: the enteric nervous system in neurological*  
521 *disorders.* *Nat Rev Gastroenterol Hepatol.* 2016;13(9):517-28.

522 45. Young HM, Bergner AJ, Muller T. *Acquisition of neuronal and glial markers by neural crest-*  
523 *derived cells in the mouse intestine.* *The Journal of comparative neurology.* 2003;456(1):1-11.

524 46. Heanue TA, Pachnis V. *Prospective identification and isolation of enteric nervous system*  
525 *progenitors using Sox2.* *Stem Cells.* 2011;29(1):128-40.

526 47. Trapnell C, Cacchiarelli D, Grimsby J, Pokharel P, Li S, Morse M, et al. *The dynamics and*  
527 *regulators of cell fate decisions are revealed by pseudotemporal ordering of single cells.* *Nature*  
528 *Biotechnology.* 2014;32(4):381-6.

529 48. Okamura Y, Saga Y. *Notch signaling is required for the maintenance of enteric neural crest*  
530 *progenitors.* *Development.* 2008;135(21):3555-65.

531 49. Moore RE, Clarke J, Alexandre P. *Protrusion-Mediated Signaling Regulates Patterning of the*  
532 *Developing Nervous System.* *Front Cell Dev Biol.* 2020;8:579073.

533 50. Harrison C, Wabbersen T, Shepherd IT. *In vivo visualization of the development of the enteric*  
534 *nervous system using a Tg(-8.3bphox2b:Kaede) transgenic zebrafish.* *Genesis.* 2014;52(12):985-90.

535 51. Sang-Yeob Y, MinJung K, Hyung-Seok K, Tae-Lin H, Ajay BC. *Fluorescent protein expression*  
536 *driven by her4 regulatory elements reveals the spatiotemporal pattern of Notch signaling in the*  
537 *nervous system of zebrafish embryos.* *Developmental Biology.* 2007;301(2):555-67.

538 52. Raymond PA, Barthel LK, Bernardos RL, Perkowsky JJ. *Molecular characterization of retinal*  
539 *stem cells and their niches in adult zebrafish.* *BMC Developmental Biology.* 2006;6(1):36.

540 53. Miyasaka N, Morimoto K, Tsubokawa T, Higashijima S-i, Okamoto H, Yoshihara Y. *From the*  
541 *Olfactory Bulb to Higher Brain Centers: Genetic Visualization of Secondary Olfactory Pathways in*  
542 *Zebrafish.* *The Journal of Neuroscience.* 2009;29(15):4756-67.

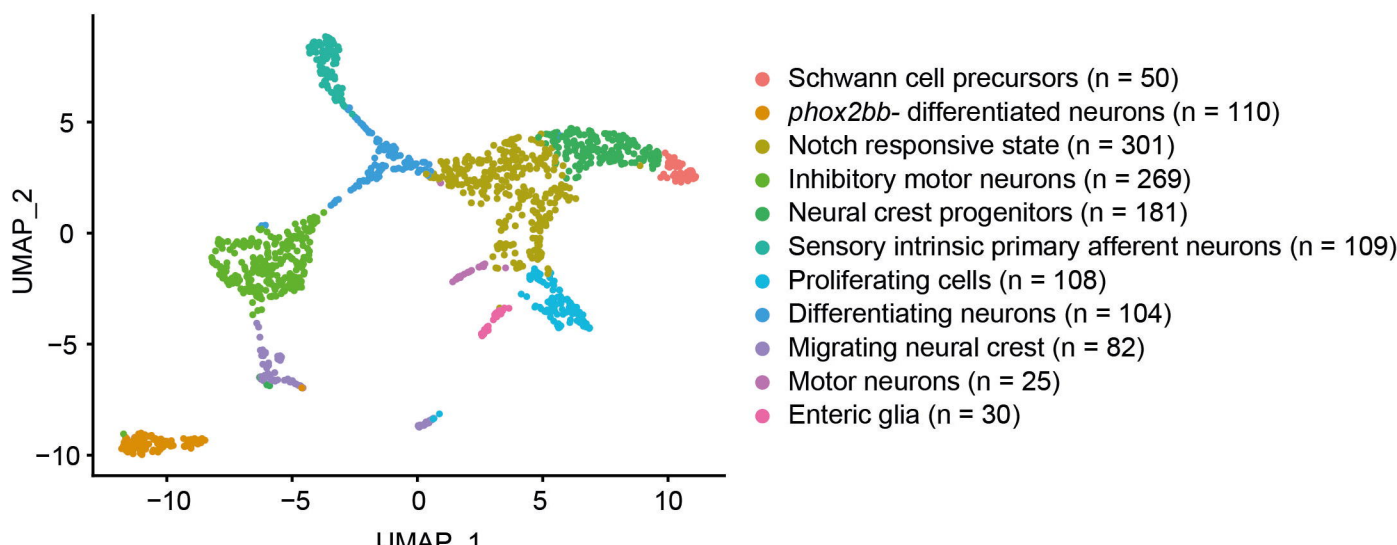
543 54. Satou C, Kimura Y, Hirata H, Suster ML, Kawakami K, Higashijima S-i. *Transgenic tools to*  
544 *characterize neuronal properties of discrete populations of zebrafish neurons.* *Development.*  
545 2013;140(18):3927-31.

546 55. Stuart T, Butler A, Hoffman P, Hafemeister C, Papalexi E, Mauck WM, III, et al. *Comprehensive*  
547 *Integration of Single-Cell Data.* *Cell.* 2019;177(7):1888-902.e21.

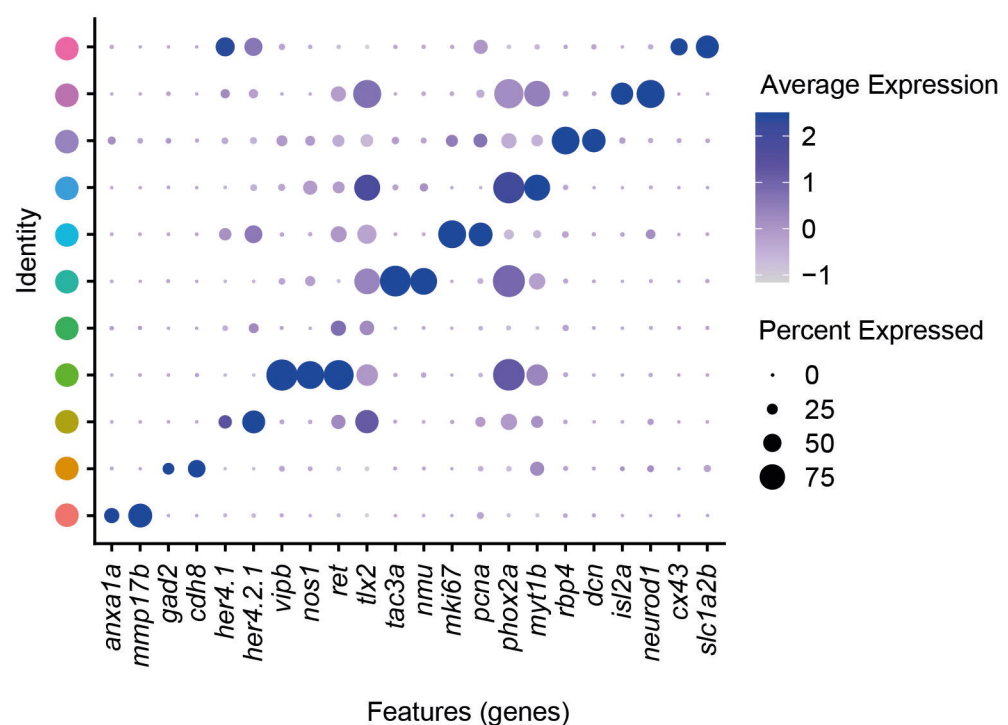
548 56. Kuil LE, Oosterhof N, Ferrero G, Mikulášová T, Hason M, Dekker J, et al. *Zebrafish*  
549 *macrophage developmental arrest underlies depletion of microglia and reveals Csf1r-independent*  
550 *metaphocytes.* *eLife.* 2020;9:e53403.

551 57. Heanue TA, Boesmans W, Bell DM, Kawakami K, Vanden Berghe P, Pachnis V. *A Novel*  
552 *Zebrafish ret Heterozygous Model of Hirschsprung Disease Identifies a Functional Role for mapk10 as*  
553 *a Modifier of Enteric Nervous System Phenotype Severity.* *PLoS Genet.* 2016;12(11):e1006439.

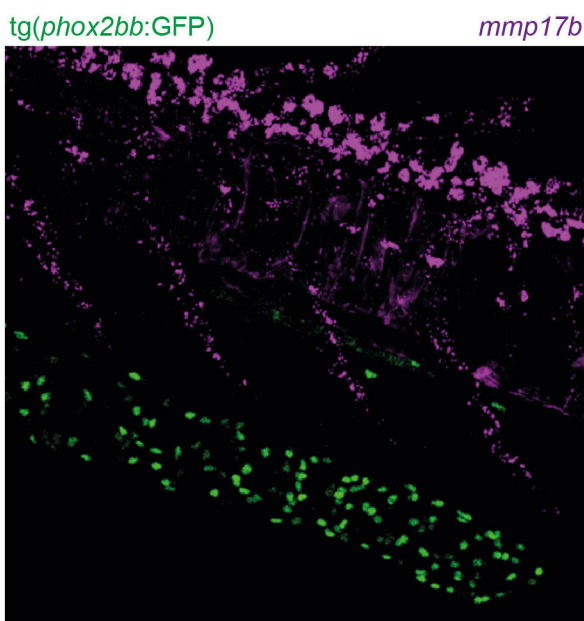
554 58. Hyland C, Mfarej M, Hiotis G, Lancaster S, Novak N, Iovine MK, et al. *Impaired Cx43 gap*  
555 *junction endocytosis causes morphological and functional defects in zebrafish.* *Mol Biol Cell.*  
556 2021;32(20):ar13.



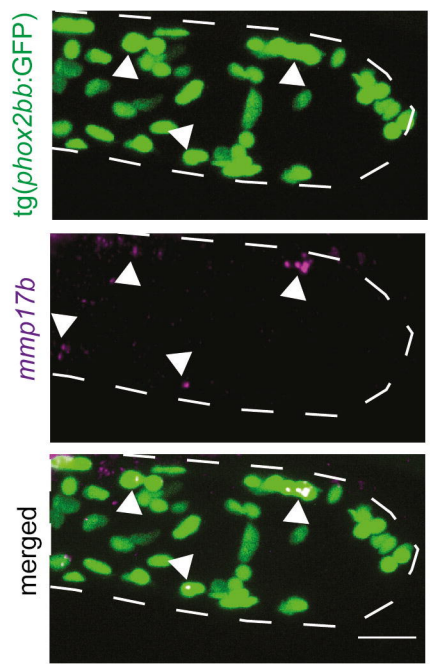
B

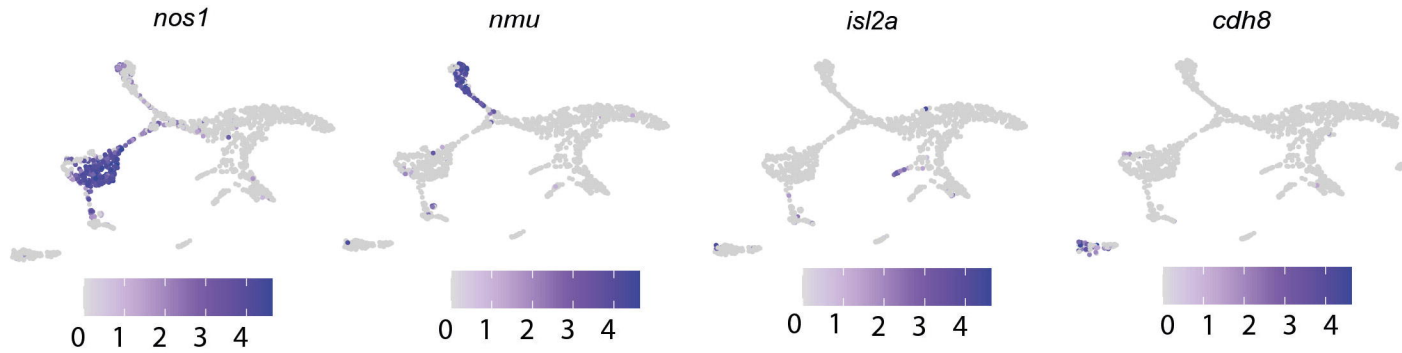
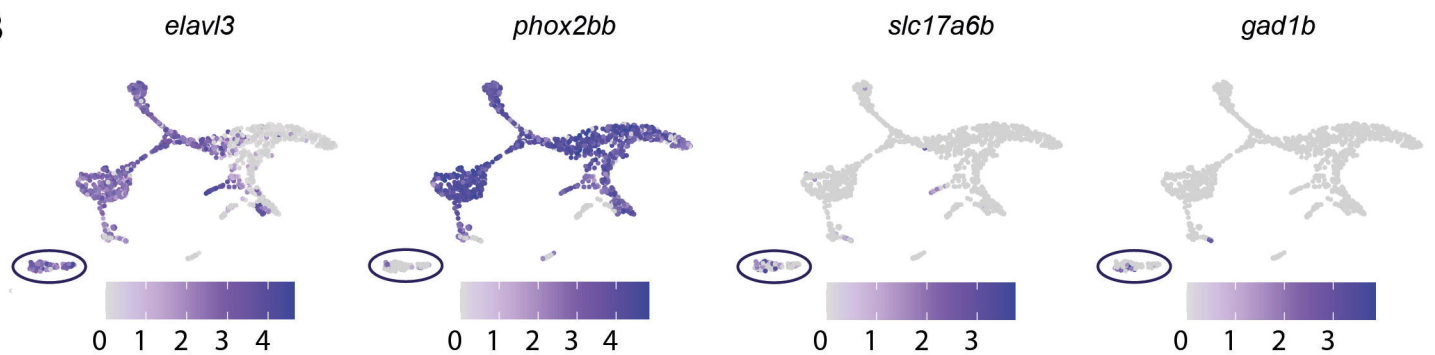
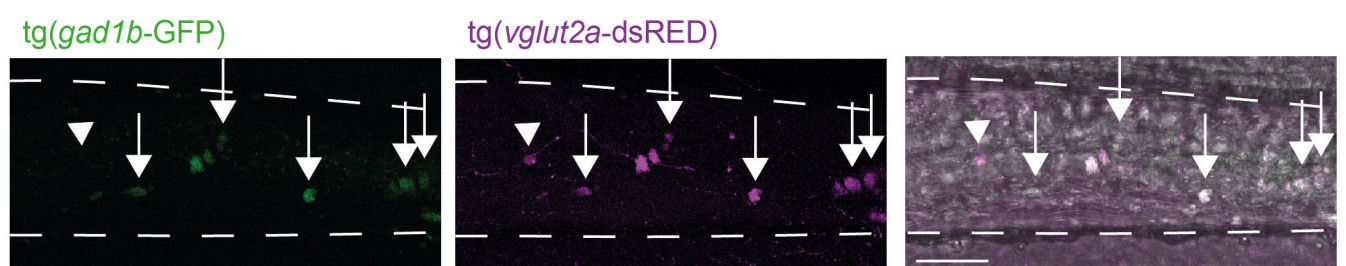
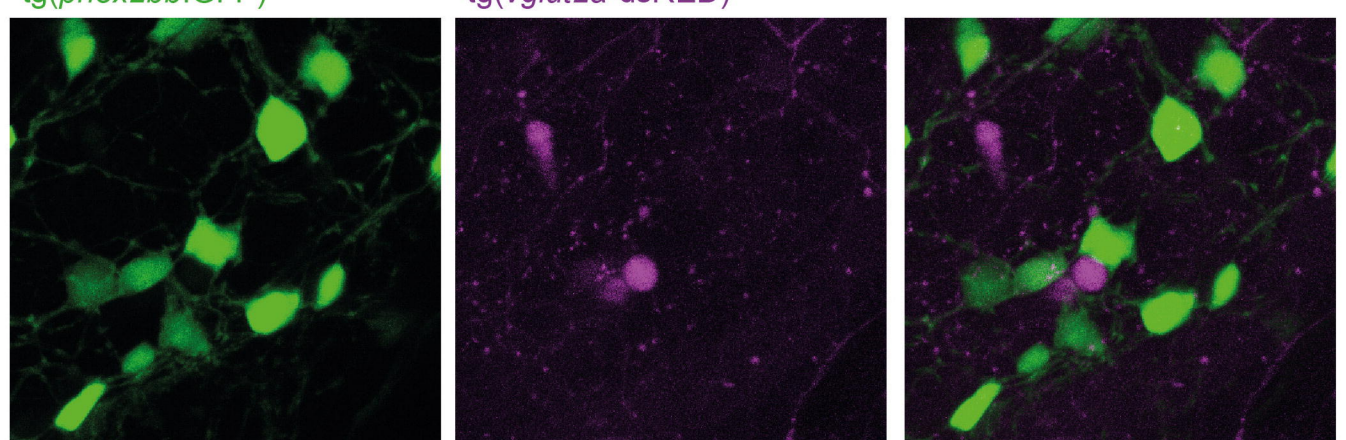


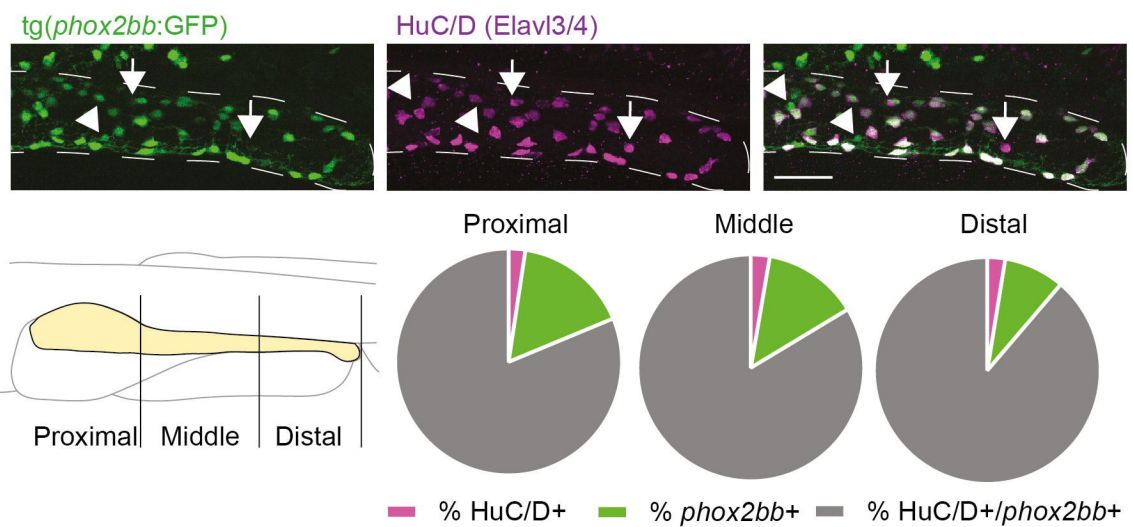
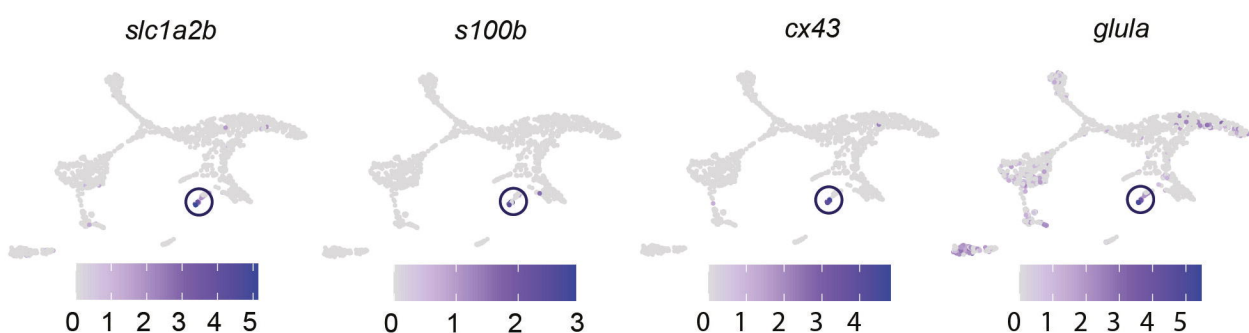
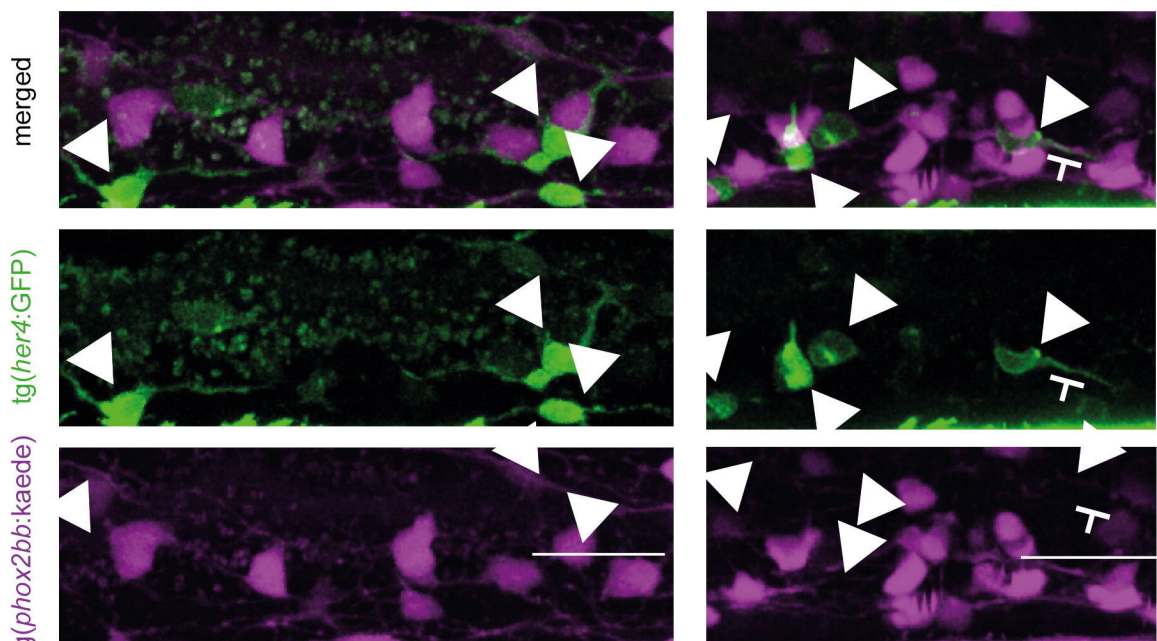
C

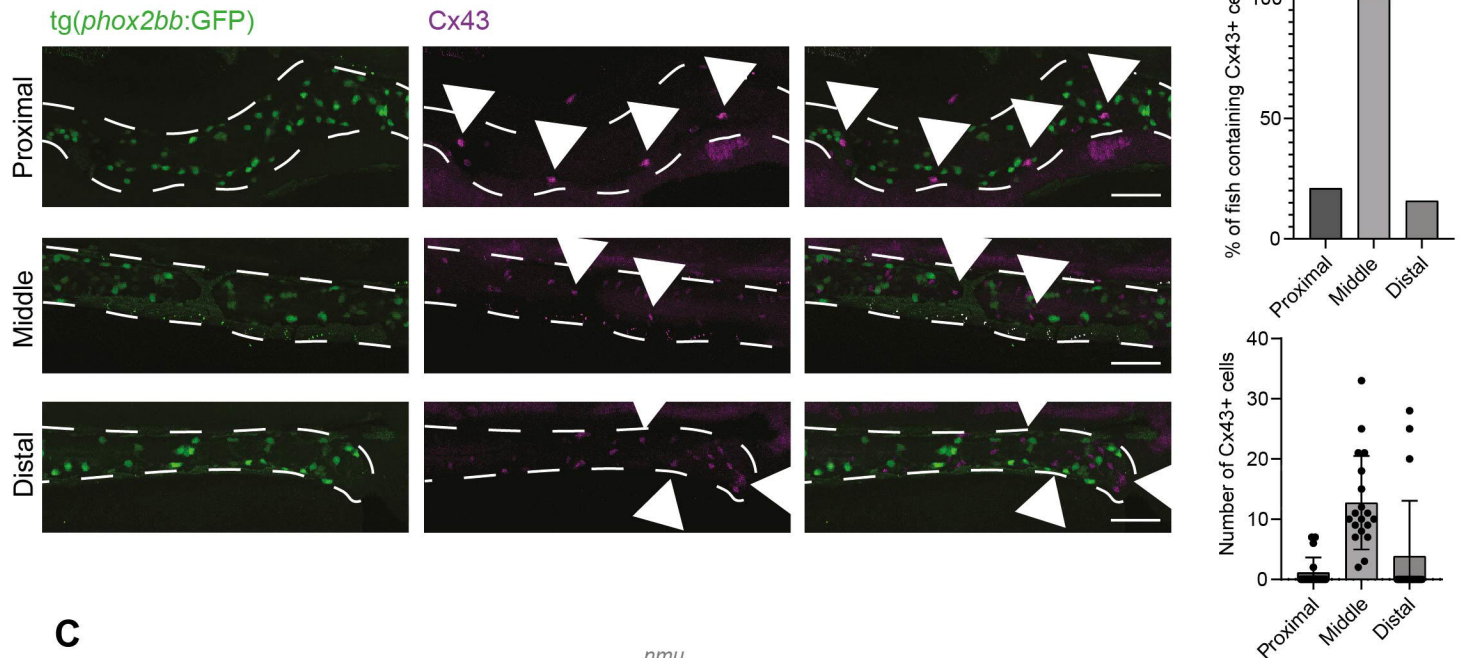


D

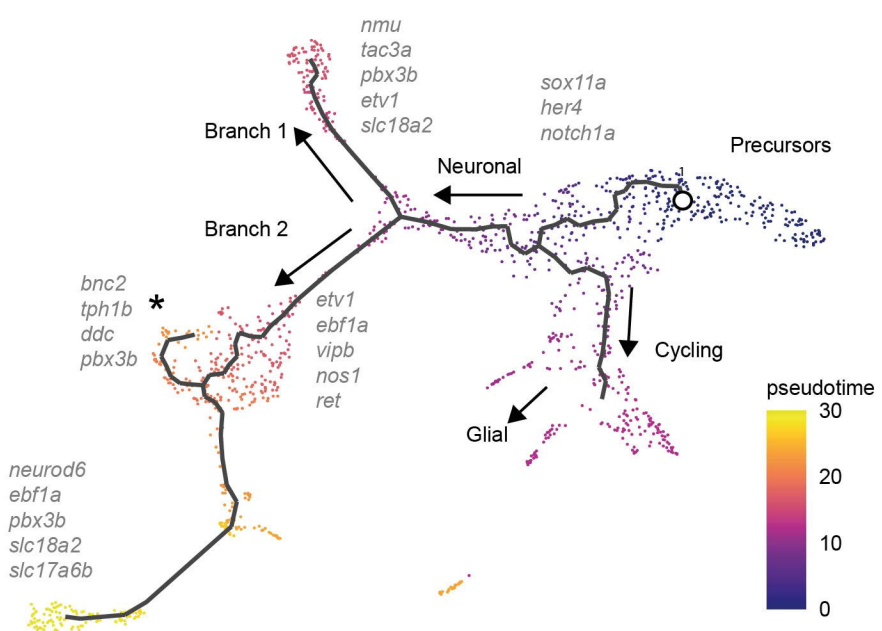


**A****B****C****D**

**A****B****C**



**C**



**D**

